EUROPEAN SYNCHROTRON RADIATION FACILITY

INSTALLATION EUROPEENNE DE RAYONNEMENT SYNCHROTRON

Experiment Report Form

The double page inside this form is to be filled in by all users or groups of users who have had access to beam time for measurements at the ESRF.

Once completed, the report should be submitted electronically to the User Office via the User Portal:
https://wwws.esrf.fr/misapps/SMISWebClient/protected/welcome.do

Deadlines for submission of Experimental Reports

Experimental reports must be submitted within the period of 3 months after the end of the experiment.

Experiment Report supporting a new proposal ("relevant report")

If you are submitting a proposal for a new project, or to continue a project for which you have previously been allocated beam time, you must submit a report on each of your previous measurement(s):

- even on those carried out close to the proposal submission deadline (it can be a *"preliminary report"),*
- even for experiments whose scientific area is different form the scientific area of the new proposal,
- carried out on CRG beamlines.

You must then register the report(s) as "relevant report(s)" in the new application form for beam time.

Deadlines for submitting a report supporting a new proposal

- 1st March Proposal Round - **5th March**
- 10th September Proposal Round - **13th September**

The Review Committees reserve the right to reject new proposals from groups who have not reported on the use of beam time allocated previously.

Reports on experiments relating to long term projects

Proposers awarded beam time for a long term project are required to submit an interim report at the end of each year, irrespective of the number of shifts of beam time they have used.

Published papers

All users must give proper credit to ESRF staff members and proper mention to ESRF facilities which were essential for the results described in any ensuing publication. Further, they are obliged to send to the Joint ESRF/ ILL library the complete reference and the abstract of all papers appearing in print, and resulting from the use of the ESRF.

Should you wish to make more general comments on the experiment, please note them on the User Evaluation Form, and send both the Report and the Evaluation Form to the User Office.

Instructions for preparing your Report

- fill in a separate form for each project or series of measurements.
- type your report in English.
- include the experiment number to which the report refers.
- make sure that the text, tables and figures fit into the space available.
- if your work is published or is in press, you may prefer to paste in the abstract, and add full reference details. If the abstract is in a language other than English, please include an English translation.

ESRF	**Experiment title:** Characterisation of Chikungunya non-structural protein 1 (nsP1) complexes using cryo EM	**Experiment number**: Mx2178
Beamline: CM01	**Date of experiment**: from: 09/08/19 to: 12/08/19	**Date of report**: 20/04/20
Shifts: 9	**Local contact(s)**: Eaazhisai Kandiah	*Received at ESRF:*

Names and affiliations of applicants (* indicates experimentalists):

Rhian Jones*

Juan Reguera*

Report: Three replicate nsP1 grids (carbon coated, Cu/Rh 300 mesh Quantifoil R2/2 holey) that had been pre-screened on the TALOS Artica at the CNB Madrid were loaded into the microscope by Eaazhisai. The first grid was determiend to be of sufficient quality for data collection, and the first few hours of the experiment were dedicated to screening grid squares for optimal ice thickness and optimisation of acquisition parameters. Specifically, the dose per frame ($0.96e^-/Å^2$-$1.5e^-/Å^2$) and total exposure time (5-9s) were varied to determine whether this could improve contrast close to focus; a problem that we commonly encounter in nsP1 data collections due to the presence of detergent in the sample buffer and compounded by the continuous carbon film over the grid. Contrast in the images was good until around 0.8μm.

The following acquisition parameters were selected for the final experiment: nominal magnification: 165,000x (corresponding to a pixel size of 0.827Å/pix), spot size: 6, defocus range: 1-2.5μm, dose rate: $5.27e^-$/pix/s, exposure time: 5s distributed over 40 frames, total dose per movie: $38.5e^-/Å^2$. The energy filter was set at a slit width of 20eV. Using FEI EPU automated software, 5626 movies were recorded in couting mode from 11 grid squares that had been selected at the screening stage, where seven images were aquired per hole. Drift

correction was set once per grid square, and autofocussing performed every third grid hole. The movies were processed on the fly using the CM01 pipeline; monitored via the ExiMX interface. Movie drift was first corrected using MotionCorr2 and CTF correction performed with gCTF. The images exhibited minimal drift (Figure 1) over the dataset, and high overall resolution. Both factors were significantly improved compared with a previous collection from the same grid on a TALOS.

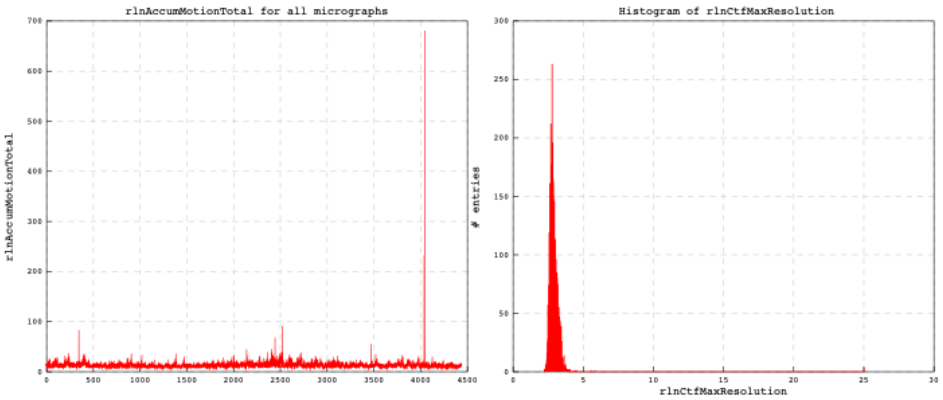

Figure 1: Plot of per-micrograph motion from MotionCorr2 (left), and histogram of maximum micrograph resolution estimated from CTFFind4 (right). Micrographs typically exhibit drift in the range of 10Å, and micrographs with very high drifts were discarded from further analysis. Most micrographs exhibit Thon rings going out to beyond 2.5-3Å.

Data were transferred to the lab, and the movies were processed from within Relion 3.0. Following motion correction (Motion Corr2) and CTF correction (CTFFind 4), 478 of the 5626 movies were discarded due to drift, ice contamination, poor contrast or highly astigmatic CTFs. Around 1000 particles in a selection of orientations were selected from 100 micrographs for 2D classification, yielding templates for Relion's autopicking procedure. From an intitial 263,415 particles selected from the dose-weighted micrographs (roughly 30-50 per micrograph), 180,921 were retained following pruning and 2D classification. 2D classification yielded classes clearly corresponding to single dodocameric rings of nsP1 (Figure 2), and double dodocameric rings (24mers, figure 2) where the two rings were separated by a micelle belt. The presence of the double and single ring species of nsP1 has previously been documented in negative stain and cryo-EM imaging. Both single and double rings exhibited a range of particle orientations corresponding well with projections from our final models, although top views were singificantly more poulated for single rings and lateral views for double rings. Despite preferential orientations, there was sufficient sampling of the symmetry space to obtain reconstructions to high resolution (Figure 2).

Whilst lateral views in 2D classes could easily be separated for double or single rings, top views could not easily be ascribed to either species by eye. 3D classification was used to separate single rings from doubles, using a low-pass filtered single ring *ab initio* model that had been obtained from a previous dataset recorded from the same grid on a TALOS. Classifications with different numbers of classes consistently yielded two

major classes corresponding to the single rings (105,825 particles) and double rings (47,338 particles), with smaller classes of "junk" partciles. A further round of 3D classification performed with the single rings improved particle homogeneity (94,018 particles). *Ab initio* model generation and 3D classification were all performed without imposing symmetry.

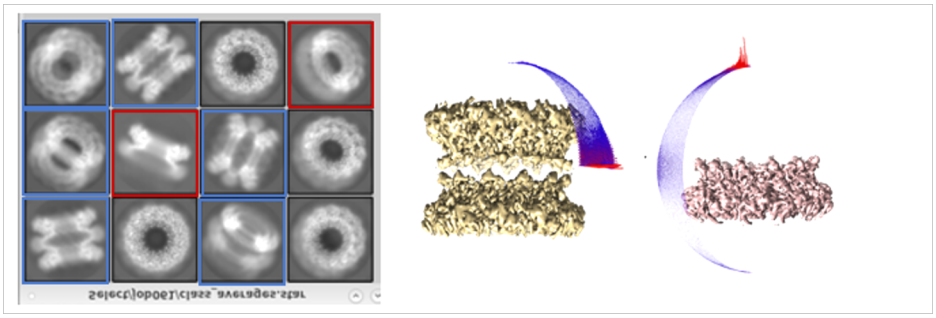

Figure 2: Particle orientations. Left: 2D classes from Relion, where lateral views corresponding to double rings and single rings are boxed in blue and red respectively. Top views could only be separated successfully via 3D classification. All rings exhibit 12 fold symmetry. Centre: D12 double ring reconstruction with plot of the number of partciles at given Euhler angles. Cylinders are longer and coloured red for more highly populated orientations. Right: the same plot for the single rings reconstructed with C12 symmetry.

Reconstructions were performed with the single and double ring classes in Relion 3Dautorefine, with the models and particles obtained from 3D classification. Reconstructions were initially performed in C1 to ascertain whether there were conformational differences between nsP1 protomers. Resolution reached 4.3Å (4.0Å post map sharpening) for the single rings and 7.1Å (6.8Å following map sharpening) for the double rings. As no significant difference was observed between protomers in the maps, **single ring reconstructions were performed imposing C12 symmetry** to a resolution of 3.7Å without masking, and 3.0Å with masking, as estimated using the gold FSC criterion at a threshold of 0.143. Resolution improved to 3.4Å and 2.9Å following map sharpening, and further to **2.6Å** following a single round of particle polishing and per-particle CTF correction. For the **double rings, reconstructions with D12 symmetry** reached a resolution of 3.87Å without masking, and 3.1Å with masking. A single round of particle polishing and per-particle CTF correction finally improved the resolution to **2.9Å**. Subsequent rounds of per-particle CTF correction and polishing did not improve resolution for either reconstruction. Both of these resolutions are significantly higher than those obtained with the TALOS dataset using the same workflow but with roughly one third of the number of particles (3.3Å for single rings- 24,554 particles, 3.8Å for double rings- 16,366 particles).

The high resolution and overall excellent quality of the maps allowed for *ab initio* modelling of the nsP1 protein sequence using Coot; an important advance as bioinformatic modelling approaches have consistently failed to correctly predict the nsP1 fold. Following iterative cycles of refinement in Phenix with NCS and model building in Coot, the entire protein sequence was built with the exception of N-terminal residues MG, loop regions 365-375 and 451-457 and C-terminal region 473-535; local resolution data suggests that map resolution in these regions is between 3-5Å. No overall differences in the structures are observed between D12 and C12 reconstructions, and as no contacts are observed between the double rings in the micelle, we assume that the single rings are the biologically relevant assembly.

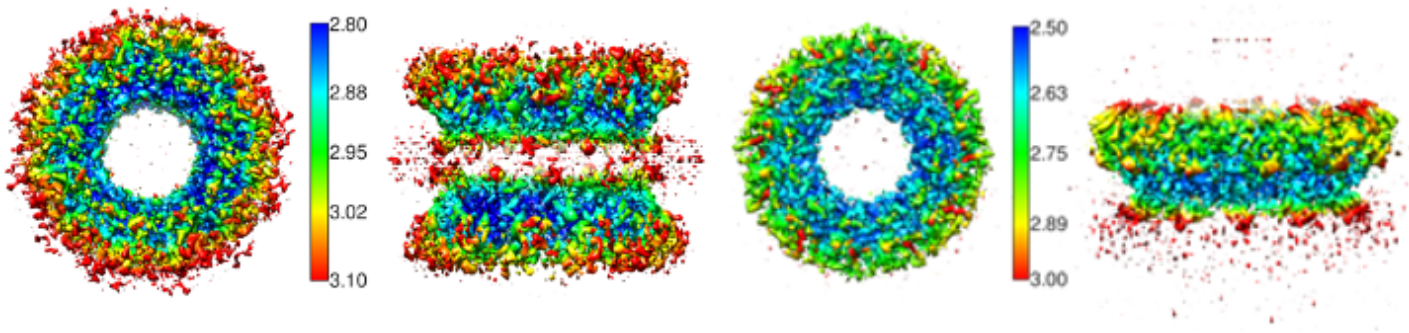

Figure 3: Final reconstructions of D12 double rings (left) and C12 single rings (right), coloured according to local resolution (keys indicated). Top and side views are presented. Resolution is worst in the region of the spikes entering the micelle (colored red) and the outer regions of the ring. Overall resolution is also lower and more narrowly distributed over the single rings, perhaps owing to an increased number of partciles in the reconstruction.

A paper describing the overall structure of nsP1 has been submitted, and we hope to publish it within the next few months. Briefly, the structure exhibits a central capping domain that is highly conserved between other N7 methyltransferases, in addition to auxillary domains that mediate pore-formation, oligomerisation between protomers and membrane binding that could not be predicted from the protein's sequence. The structure reveals an unexpected mode of membrane association, and provides a molecular rationale for the interdependence of membrane binding and complex formation. These details provide the first structural basis for the dependence of nsP1 capping activity on membrane association. In addition, the dimensions of the rings have important implications for the viral replication cycle; corresponding very well with those observed at the entrance of the membrane organelles (spherules) where alphaviral replication occurs. This structure, the first of it's kind for a +ssRNA virus, has allowed us to propose a novel role for nsP1 in alphaviral replication.

For future experiments, we hope to obtain cryo-EM structures of the nsP1 complexes in complex with capping intermediates, ssRNA, and possibly with other alphaviral nsPs. To improve future data collections, we are

currently trialling ways to improve image contrast through altering the composition of the sample buffer, and are looking for ways to separate the double and single rings during purification and prior to application to grids. We are extremely grateful to Eaazhisai for her help during data collection, and advice regarding data processing.